The type III inositol 1,4,5-trisphosphate receptor is phosphorylated by cAMP-dependent protein kinase at three sites

Matthew D. SOULSBY and Richard J. H. WOJCIKIEWICZ[1]

Department of Pharmacology, SUNY Upstate Medical University, 750 East Adams Street, Syracuse, NY 13210-2339, U.S.A.

IP_3 (inositol 1,4,5-trisphosphate) receptors form tetrameric, IP_3-gated Ca^{2+} channels in endoplasmic reticulum membranes, and are substrates for several kinases, including PKA (cAMP-dependent protein kinase). Activation of PKA has been reported to either enhance or inhibit type III IP_3 receptor Ca^{2+}-channel activity, but, as yet, the sites of phosphorylation remain unknown. Here, we reveal that PKA phosphorylates the type III IP_3 receptor at Ser^{916}, Ser^{934} and Ser^{1832}, and that, intriguingly, each site is located close to a putative surface-exposed peptide loop. Furthermore, we demonstrate that Ser^{934} is considerably more susceptible to PKA-dependent phoshorylation than either Ser^{916} or Ser^{1832}. These findings define the sites at which the type III IP_3 receptor is phosphorylated by PKA, and provide the basis for exploring the functional consequences of this regulatory event.

Key words: cAMP-dependent protein kinase, phosphorylation, type III inositol 1,4,5-trisphosphate receptor.

INTRODUCTION

IP_3 (inositol 1,4,5-trisphosphate) receptors (IP_3Rs) are a family of proteins which form Ca^{2+} channels in endoplasmic reticulum membranes, and which govern Ca^{2+} release from this organelle by opening in response to IP_3 and Ca^{2+} binding [1]. In mammals, type I, II and III IP_3Rs (IP_3R1, IP_3R2 and IP_3R3) are highly homologous, and have the same overall structure, with an N-terminal 'ligand-binding domain', a C-terminal 'channel domain', and an intervening 'coupling domain' containing putative binding sites for several regulatory factors [1,2]. Despite the structural similarities, expression of IP_3R1 to IP_3R3 varies considerably between tissues [3–5]. IP_3R1, for example, is very widely expressed, with particularly high levels in neuronal cells, whereas IP_3R2 and IP_3R3 are expressed more sporadically, but with considerable abundance, in the liver and pancreas respectively [3–7].

There are also subtle, but clear, differences in the properties of the three IP_3R types. IP_3R3, for example, has a lower affinity for IP_3 [8,9] and ATP [10,11] than IP_3R1 or IP_3R2, but is more sensitive to Ca^{2+} [11]. Furthermore, functional differences between the three receptor types have been attributed to their differential phosphorylation by PKA (cAMP-dependent protein kinase) [12–14]. To date, however, only the effects of PKA on IP_3R1 have been characterized. Two serine residues (1588 and 1755) are phosphorylated [15–17], and these modifications appear to enhance Ca^{2+} channel activity in intact cells [18]. In contrast, whereas phosphorylation of IP_3R2 [12,19] and IP_3R3 [12–14,20] may modulate Ca^{2+} channel activity, reported results have often been contradictory; for example, for IP_3R3, PKA has been suggested to have either stimulatory [13] or inhibitory [14] effects. Furthermore, nothing is currently known about the sites at which these receptors are phosphorylated.

IP_3R3 has been implicated in a variety of Ca^{2+}-dependent physiological processes. For example, it may play an important role in generating the Ca^{2+} signals that modulate glucose-stimulated insulin secretion in pancreatic β cells [7], and initiate exocytosis and electrolyte secretion in pancreatic acinar cells [20], and therefore its phosphorylation could have important physiological consequences. To provide a basis for fully understanding the functional consequences of IP_3R3 phosphorylation, we set out to define the sites at which it is phosphorylated. We report here that IP_3R3 is phosphorylated by PKA at serine residues 916, 934 and 1832, and that, intriguingly, these sites are close to putative surface-exposed peptide loops.

EXPERIMENTAL

Materials

$[^{32}P]P_i$ (H_3PO_4, carrier-free) and [γ-^{32}P]ATP (6000 Ci/mmol) were from PerkinElmer, and the PKA catalytic subunit was from Promega. All other chemicals were from Sigma. TL3, a mouse monoclonal antibody directed against N-terminal amino acids 22–230 of IP_3R3, was from BD Biosciences. CT1 and CT3, affinity-purified rabbit antisera directed against the C-termini of IP_3R1 and IP_3R3 respectively, were prepared as described previously [3].

Mutagenesis

The constructs pCWI (which encodes mouse SI+/SII + IP_3R1) and pCI_3 (which encodes rat IP_3R3; kindly given by Dr Graeme Bell, University of Chicago, IL, U.S.A.), have been described previously [7,17]. Mutagenesis of Ser^{916}, Ser^{934} and Ser^{1832} to alanine was achieved by PCR and pairs of mutagenic primers. Briefly, pCI_3 was mutated to introduce alanine at positions 934, 916 and 1832 using the primer pairs 5′-CCATGGTGCTATCGCGAAAGCAGGCTGTATTTGGTGC-3′ and 5′-GCACCAAATACAGCCTGCTTTCGCGATAGCACCATGG-3′, 5′-GCAAGAACGTGCGCAGGGCCATCCAGG-3′ and 5′-CCTGGATGGCCCTGCGCACGTTCTTGC-3′, and 5′-CCACCAAAGGACGCGTGTCCGCCTTCTCCATGC-3′ and 5′-GCATGGAGAAGGCGGACACGCGTCCTTTGGTGG-3′ respectively. These primer pairs also introduced NruI, FspI and MluI sites, respectively, to facilitate

Abbreviations used: HEK, human embryonic kidney; IP_3(R), inositol 1,4,5-trisphosphate (receptor); PKA, cAMP-dependent protein kinase; PGE_1, prostaglandin E_1; PKG, cGMP-dependent protein kinase.

[1] To whom correspondence should be addressed (email wojcikir@upstate.edu).

screening, and correct introduction of the desired mutations was confirmed by sequencing.

Phosphorylation of IP_3Rs in intact cells

Wells of HEK (human embryonic kidney) cells were transfected [17], incubated with approx. 100 μCi of [^{32}P]P_i for 2 h in 750 μl of serum-free, phosphate-free Dulbecco's modified Eagle's medium, and then stimulated to induce IP_3R phosphorylation. Cells were then solubilized with ice-cold, phosphatase-inhibitor-supplemented lysis buffer [17], and IP_3Rs were immunoprecipitated overnight at 4 °C with Protein A–Sepharose CL-4B beads and IP_3R1-specific CT1 or IP_3R3-specific CT3 [3]. Immune complexes were then washed three times and finally resuspended in 2× gel loading buffer [3].

Phosphorylation of purified IP_3R3

Transfected cells were solubilized with ice-cold, phosphatase-inhibitor-supplemented lysis buffer, IP_3R3s were immunoprecipitated, and *in vitro* phosphorylation of the purified receptors was then performed in 200 μl of phosphorylation buffer [12] supplemented with approx. 20 μCi of [γ-^{32}P]ATP, 5 μM non-radioactive ATP and 40 units of PKA catalytic subunit for 15 min at 30 °C. The immune complexes were then washed three times with ice-cold phosphorylation buffer supplemented with 1 mM ATP, and finally resuspended in 2× gel loading buffer.

Chymotrypsin treatment of purified IP_3R3

IP_3R3 immune complexes were washed twice with ice-cold 20 mM Tris/HCl, pH 8.0, containing 120 mM KCl and 1 mM EDTA, and were then resuspended in the same buffer supplemented with 1 μg/ml α-chymotrypsin (Type I-S) and incubated at 25 °C for the indicated times, before the addition of 4× gel loading buffer.

Electrophoresis, staining and autoradiography

IP_3R1 ($\approx$270 kDa) and IP_3R3 ($\approx$260 kDa) were electrophoresed and stained with Coomassie Blue [3], and associated radioactivity was assessed initially by autoradiography of dried gels, and then quantified by excision and scintillation counting of the radioactive bands [17].

RESULTS AND DISCUSSION

Identification of phosphorylation sites on IP_3R3

To identify sites phosphorylated by PKA, wild-type and mutant IP_3R3s were expressed in HEK cells and endogenous PKA was activated by exposing the cells to a maximally effective dose of PGE_1 (prostaglandin E_1), an approach we have used previously to analyse PKA-mediated IP_3R1 phosphorylation [17]. We mutated 33 serine and 18 threonine residues at sites resembling the PKA consensus sequences R(R/K)X(S/T), RX_2(S/T) or RX(S/T) [21]. As shown in Figure 1(A), we found that mutation of Ser^{916}, Ser^{934} and Ser^{1832} suppressed PGE_1-induced phosphorylation of IP_3R3. In comparison with wild-type receptor (IP_3R3^{SSS}; lane 4), phosphorylation of IP_3R3 mutated at Ser^{916} (IP_3R3^{ASS}; lane 6) or Ser^{1832} (IP_3R3^{SSA}; lane 10) was reduced by approx. 25 %, whereas phosphorylation of IP_3R3 mutated at Ser^{934} (IP_3R3^{SAS}; lane 8) was reduced by approx. 50 %. Furthermore, phosphorylation of IP_3R3 mutated at both Ser^{916} and Ser^{934} (IP_3R3^{AAS}; lane 12) reduced phosphorylation by approx. 75 %, and mutation of all three serine residues (IP_3R3^{AAA}; lane 14) completely abolished

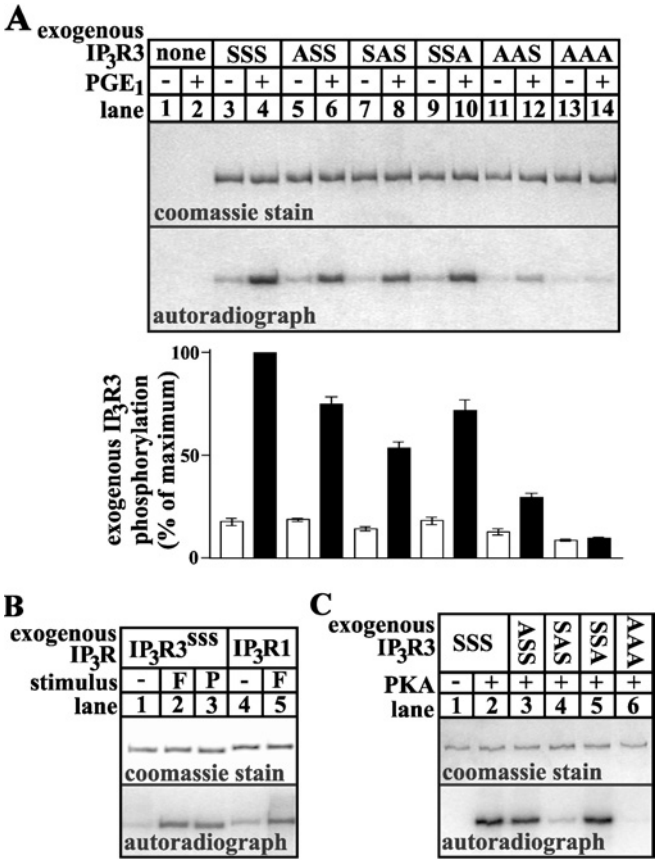

Figure 1 Site specificity of PKA-mediated IP_3R3 phosphorylation

(**A**) ^{32}P-labelled cells transfected with empty vector (lanes 1 and 2), or IP_3R3 cDNAs encoding wild-type receptor (IP_3R3^{SSS}; lanes 3 and 4), or receptors with mutations to alanine at Ser^{916} (IP_3R3^{ASS}; lanes 5 and 6), Ser^{934} (IP_3R3^{SAS}; lanes 7 and 8), Ser^{1832} (IP_3R3^{SSA}; lanes 9 and 10), Ser^{916} and Ser^{934} (IP_3R3^{AAS}; lanes 11 and 12), or Ser^{916}, Ser^{934} and Ser^{1832} (IP_3R3^{AAA}; lanes 13 and 14) were exposed to 1 μM PGE_1 for 5 min as indicated, and IP_3R3s were immunoprecipitated, electrophoresed and assessed for staining capacity (upper panel) and associated radioactivity (lower panel). Exogenous IP_3R3 phosphorylation (histogram; means $\pm$ S.E.M., $n \geqslant 3$) was calculated by subtracting radioactivity associated with endogenous IP_3R3s (lanes 1 and 2) from that in lanes 3–14, and is expressed as a percentage of the radioactivity associated with IP_3R3^{SSS} in the presence of PGE_1 (lane 4). (**B**) ^{32}P-labelled cells transfected with IP_3R3 (lanes 1–3) or IP_3R1 (lanes 4 and 5) cDNA were exposed to 1 μM PGE_1 (P) or 10 μM forskolin (F) for 5 min as indicated, and IP_3R phosphorylation was visualized as in (**A**). (**C**) IP_3R3s were immunoprecipitated from non-stimulated transfected cells and were phosphorylated with PKA catalytic subunit *in vitro*. The approx. 200–300 kDa region of gels are shown in (**A**), (**B**) and (**C**), and represent typical data from at least two independent experiments.

PGE_1-induced phosphorylation. Therefore, under conditions of maximal PKA activation, Ser^{916}, Ser^{934} and Ser^{1832} represent the entire complement of sites phosphorylated by PKA. The fidelity of this mutagenic approach is demonstrated by the fact that IP_3R3 phosphorylation was unaffected by mutations at several other consensus phosphorylation sites (e.g. at Thr^{2201} and Ser^{2483}), and at sites close to Ser^{916}, Ser^{934} and Ser^{1832} (e.g. at Ser^{1831}, which lies adjacent to Ser^{1832}, and at Ser^{925} and Ser^{930}, which lie between Ser^{916} and Ser^{934}; results not shown).

We next sought to validate our results by demonstrating that the data in Figure 1(A) represent efficient phosphorylation of the majority of exogenous IP_3R3s, rather than modification of an insignificant fraction of receptors. Figure 1(B) demonstrates that 1 μM PGE_1 elicited maximal IP_3R3 phosphorylation, since its effects (lane 3) were equal to those of 10 μM forskolin (lane 2), which maximally activates adenylate cyclase and PKA in HEK cells [22]. Importantly, IP_3R3 (lane 2) was phosphorylated with a

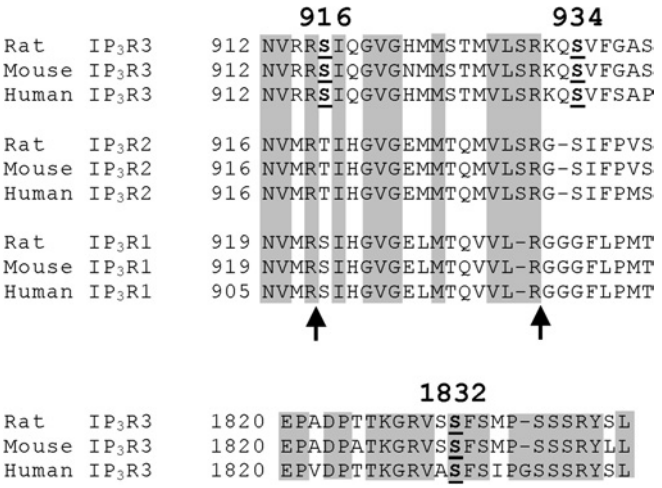

Figure 2 Amino acid sequences surrounding Ser[916], Ser[934] and Ser[1832]

Rat [7], mouse [23] and human [5,6] IP_3R1, IP_3R2 and IP_3R3 amino acid sequences were aligned and examined for regions of identity (shaded areas). The IP_3R1 and IP_3R2 sequences corresponding to the 1832 region of IP_3R3 are not shown, as these possessed no significant identity. Ser[916], Ser[934] and Ser[1832] of IP_3R3 are emboldened and underlined, and the sites at which trypsin cleaves IP_3R1 [24] are indicated by arrows.

stoichiometry similar to that seen for IP_3R1 (lane 5), which contains two well-characterized PKA phosphorylation sites and which, under these experimental conditions, incorporates at least 1 mol of phosphate/mol of receptor [17]. Thus IP_3R3s are phosphorylated with high efficiency under these conditions.

To explore IP_3R3 phosphorylation further, immunopurified receptors were phosphorylated with the catalytic subunit of PKA *in vitro* (Figure 1C). Surprisingly, whereas mutation of Ser[934] reduced PKA-mediated phosphorylation by approx. 80% (IP_3R3^{SAS}; lane 4), mutation of either Ser[916] (IP_3R3^{ASS}; lane 3) or Ser[1832] (IP_3R3^{SSA}; lane 5) had little or no effect on PKA-mediated phosphorylation, indicating that Ser[934] is the only site efficiently phosphorylated *in vitro*. Thus IP_3R3, like IP_3R1 [17], is phosphorylated differently *in vitro* than in intact cells. This discrepancy may reflect the absence of regulatory factors *in vitro*, or alteration of IP_3R3 structure following immunopurification, and reinforces the need for caution when assessing protein phosphorylation on the basis of *in vitro* experiments.

Conservation of phosphorylation sites in IP_3R3

Analysis of the sequences surrounding Ser[916], Ser[934] and Ser[1832] (Figure 2) reveals that these serine residues, and the adjacent amino acids likely to specify PKA-mediated phosphorylation, are almost completely conserved between rodent and human IP_3R3s, indicating that the results obtained herein for rat IP_3R3 can be extrapolated to human receptors. Furthermore, the 916/934 region is very well conserved between IP_3Rs 1 to 3, whereas the 1832 region is not conserved at all. Intriguingly, despite the overall conservation of the 916/934 region, the two PKA consensus sequences in IP_3R3 are not retained in IP_3R2 or IP_3R1. This is consistent with existing knowledge of IP_3R1 phosphorylation by PKA, which occurs only at Ser[1588] and Ser[1755] [15–17], and suggests that IP_3R2 will not be phosphorylated in the 916/934 region. It is also interesting to note that, in IP_3R1, two sites particularly sensitive to proteolysis by trypsin are within the 916/934 region [24] (Figure 2, arrows). Furthermore, the 1832 region lies immediately N-terminal to an additional trypsin cleavage site in IP_3R1 (within approx. 25 amino acids) [24]. These protease-sensitive sites in IP_3R1 have been proposed to be surface-exposed

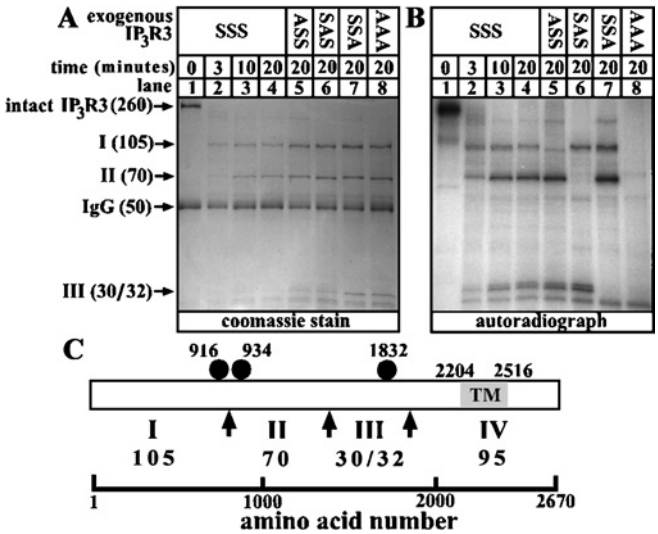

Figure 3 Chymotrypsin treatment of phosphorylated IP_3R3

^{32}P-labelled cells transfected with IP_3R3 cDNA were exposed to 1 μM PGE_1 for 5 min, and IP_3R3s were immunoprecipitated, digested with 1 μg/ml α-chymotrypsin for the times indicated, and electrophoresed. (**A**) Coomassie Blue stain showing IP_3R3 fragments in kDa generated upon digestion. (**B**) Autoradiograph of the stained gel showing radioactivity associated with each IP_3R3 fragment. (**C**) Schematic demonstrating the proximity of phosphorylation sites (closed circles) to the proposed sites of chymotrypsin-mediated cleavage (arrows) and the fragments (I–IV; size givens in kDa) generated. The transmembrane (TM) region of IP_3R3, spanning amino acids 2204–2516, is shaded.

loops, as opposed to tightly folded regions that are resistant to proteolysis [10,24]. The corresponding regions in IP_3R3, therefore, may also be exposed loops.

Chymotrypsin treatment of IP_3R3

To examine whether the 916/934 region of IP_3R3 is a protease-sensitive, surface-exposed loop, we immunoprecipitated phosphorylated IP_3R3s from HEK cells and subjected them to partial proteolysis with chymotrypsin. It has been shown previously that chymotrypsin cleaves baculovirus-generated IP_3R3 into four pieces (fragments I–IV) that migrate at 105, 70, 35 and 95 kDa respectively [10]. Our data confirm this finding, since we obtained fragments at 105 kDa, 70 kDa and 30/32 kDa when wild-type or mutant IP_3R3s were cleaved (Figure 3A). Surprisingly, a 95 kDa fragment (IV) was not detected by Coomassie Blue staining (Figure 3A), apparently because it was rapidly degraded; low amounts of this fragment, however, were detectable at early time points by immunoblotting with the C-terminus-directed antibody CT3 [3] (results not shown). Similarly, the 105 kDa fragment (I) was confirmed to be the receptor's N-terminus by immunoblotting with TL3 (results not shown). Note that, although the absolute amounts of fragments I, II and III were slightly higher for the mutant IP_3R3s (lanes 5–8) than for wild-type IP_3R3 (lane 4) (due to variation in receptor expression level), the relative abundance of fragments I, II and III appeared to be constant for each receptor, indicating that the mutations do not have a significant effect on proteolysis. Analysis of the extent to which the fragments were phosphorylated (Figure 3B) showed that, for wild-type IP_3R3 (IP_3R3^{SSS}; lanes 1–4), fragments I, II and III were all phosphorylated (lanes 2–4), that mutation of Ser[916] (IP_3R3^{ASS}; lane 5) abolished phosphorylation of fragment I, that mutation of Ser[934] (IP_3R3^{SAS}; lane 6) abolished phosphorylation of fragment II, that mutation of Ser[1832] (IP_3R3^{SSA}; lane 7) abolished phosphorylation of fragment III, and that mutation of the three serine residues (IP_3R3^{AAA}; lane 8) abolished phosphorylation of

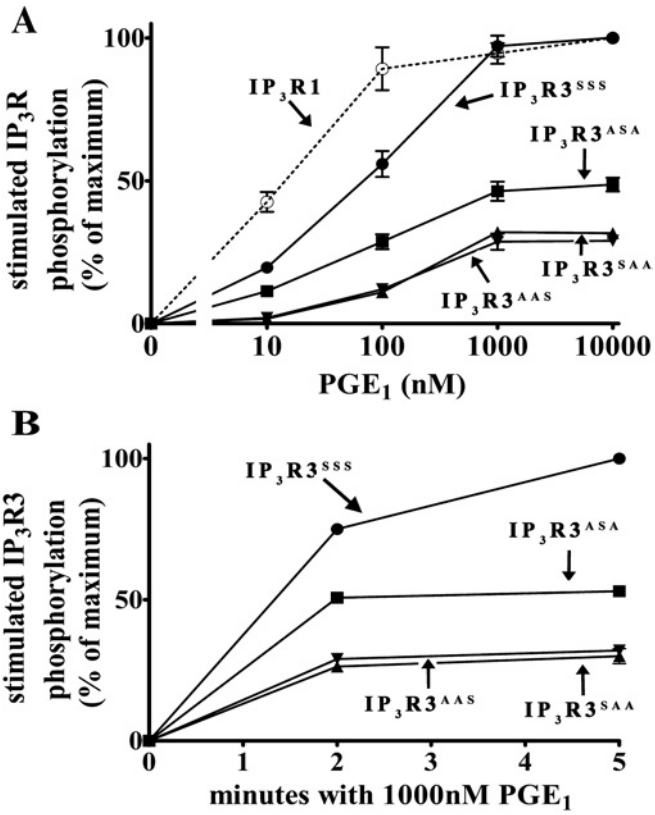

Figure 4 Ser^{934} is preferentially phosphorylated by PKA

^{32}P-labelled cells transfected with cDNA encoding IP_3R1 (○), IP_3R3^{SSS} (●), IP_3R3^{SAA} (▲), IP_3R3^{ASA} (■), or IP_3R3^{AAS} (▼) were exposed to PGE_1 as indicated. (**A**) Dose-dependence of phosphorylation after 5 min incubations. (**B**) Time course of phosphorylation. Stimulated IP_3R phosphorylation was calculated by subtracting radioactivity associated with IP_3Rs in the absence of PGE_1 and is expressed as a percentage of the radioactivity associated with wild-type IP_3Rs in the presence of 10 μM (**A**) or 1 μM (**B**) PGE_1 (means ± S.E.M., $n \geqslant 3$; error bars may be occluded by symbols).

fragments I, II and III. Furthermore, and importantly, mutation of any one site did not diminish phosphorylation of the other two sites, indicating that phosphorylation at Ser^{916}, Ser^{934} and Ser^{1832} are independent events. These data lead to the model shown in Figure 3(C), in which the chymotrypsin cleavage site that separates fragments I and II lies between Ser^{916} and Ser^{934}. The exact cleavage site could not be determined, however, as chymotrypsin cuts at the C-terminal side of residues with large hydrophobic side chains [25], and several of these are present between Ser^{916} and Ser^{934}. Overall, these data indicate that the 916/934 region is a surface-exposed loop and, since this region is so well conserved among IP_3Rs 1 to 3, suggest that it may be critical to receptor function. It is likely to be especially important in IP_3R3 regulation, as it contains two PKA phosphorylation sites.

PKA preferentially phosphorylates Ser^{934}

Since Ser^{934} contributed more to overall IP_3R3 phosphorylation than Ser^{916} or Ser^{1832} under conditions of maximal PKA activation (Figures 1A and 3B), we sought to determine whether the three sites differed in their sensitivity to PKA. To do this, we measured the amount of phosphorylation in IP_3R3s containing only Ser^{916} (IP_3R3^{SAA}), Ser^{934} (IP_3R3^{ASA}) or Ser^{1832} (IP_3R3^{AAS}) in response to a range of PGE_1 concentrations. Figures 4(A) and 4(B) show that Ser^{934} was phosphorylated approximately twice as much as that of Ser^{916} or Ser^{1832} at all doses of PGE_1 and

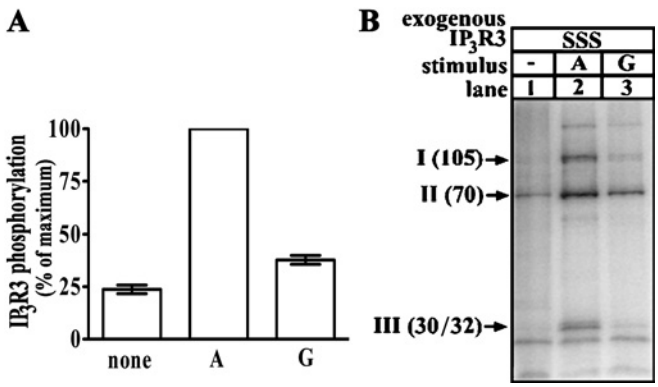

Figure 5 Effects of PKG activation

^{32}P-labelled cells transfected with cDNA encoding wild-type IP_3R3 were exposed to 1 mM 8-bromo-cAMP (A) or 8-bromo-cGMP (G) for 30 min, as indicated. (**A**) IP_3R3 phosphorylation expressed as a percentage of the radioactivity associated with IP_3R3 in the presence of 8-bromo-cAMP (means ± S.E.M., $n = 5$). (**B**) Autoradiograph of phosphorylated IP_3R3 fragments generated as in Figure 3.

at all times tested, and that all three sites were phosphorylated maximally within 2 min. Furthermore, Figure 4(A) demonstrates that Ser^{934} was slightly more sensitive to PGE_1 than Ser^{916} or Ser^{1832}, since EC_{50} values for PGE_1 were approx. 60, 130 and 130 nM for Ser^{934}, Ser^{916} and Ser^{1832} respectively. Taken together, these data indicate that PKA preferentially phosphorylates Ser^{934}. The reasons for this remain unknown, but could be due to several factors. First, the structure of IP_3R3 could account for the differences in phosphorylation. Ser^{934} may simply be more accessible to PKA, and thus be more readily phosphorylated than Ser^{916} or Ser^{1832}. Although this may explain why Ser^{934} is phosphorylated more readily than Ser^{1832}, it does not explain why Ser^{934} would be more sensitive to PKA than Ser^{916}, since they are in such close proximity. A better explanation may be found in the sequences surrounding the phosphorylation sites. Ser^{934}, in the sequence RKQ**S**, falls within the optimal PKA consensus sequence R(R/K)X(**S**/T), whereas Ser^{916}, in the sequence RR**S**, and Ser^{1832}, in the sequence RVS**S**, fall within less optimal consensus sequences [21].

Interestingly, whereas Figure 1(B) shows that wild-type IP_3R1 and IP_3R3 are phosphorylated equally under conditions of maximal PKA activation, Figure 4(A) indicates that IP_3R1 is ≈5-fold more sensitive to PKA than is IP_3R3, since EC_{50} values for PGE_1 were approx. 15 and 75 nM for IP_3R1 and IP_3R3 respectively. The reason behind this difference remains unknown. It could be due to a type-specific regulatory protein, such as a PKA-anchoring protein, an example of which has been shown to associate with IP_3R1, but not IP_3R3 [26]. Alternatively, it could be due to the fact that only one site (Ser^{934}) in IP_3R3 falls within the optimal PKA consensus sequence R(R/K)X(**S**/T) [21], whereas both PKA-dependent phosphorylation sites in IP_3R1 (Ser^{1588} and Ser^{1755}) meet this requirement. Regardless of the reasons, this difference should be taken into account when examining the functional effects of IP_3R phosphorylation in systems that express both receptor types. This is especially important, considering that IP_3R1 and IP_3R3 are often co-expressed [3,4], that heterotetrameric IP_3R channels readily form in intact cells [1,3,4], and that PKA may have different functional effects on IP_3R1 and IP_3R3.

Phosphorylation of IP_3R3 by PKG (cGMP-dependent protein kinase)

Finally, we sought to define the effects of PKG, since PKA and PKG share similar consensus sequences [21] and both can

phosphorylate IP_3R1 [16,17] in intact cells. Activation of PKG with 8-bromo-cGMP (Figure 5A) resulted in a slight increase in IP_3R3 phosphorylation, approx. 20 % of that seen when PKA was activated with 8-bromo-cAMP. Similarly to PKA, although there was some PKG-dependent phosphorylation on fragments I (Ser^{916}) and III (Ser^{1832}), the majority of phosphorylation occurred on fragment II (Ser^{934}; Figure 5B). The effects of 8-bromo-cGMP were not due to 'cross-activation' of PKA, since that does not occur under these conditions [17]. We conclude, therefore, that PKG phosphorylates IP_3R3 predominately at Ser^{934}, but with significantly less efficiency than PKA.

Conclusions

In summary, we have determined that PKA phosphorylates IP_3R3 at Ser^{916}, Ser^{934} and Ser^{1832} in an independent manner, and that each site is located at or close to a putative surface-exposed loop. Further, we have shown that Ser^{934} is preferentially phosphorylated, that IP_3R1 is $\approx$5-fold more sensitive to PKA-dependent phosphorylation than IP_3R3, and that PKG phosphorylates IP_3R3, but with significantly less efficiency than PKA. This is the first study to address the sites of cyclic-nucleotide-dependent phosphorylation of IP_3R3, and provides a basis for studying the functional consequences of this regulatory event.

We thank Dr D. I. Yule, Dr M. L. Vallano, Dr S. Blystone, K. Alzayady and M. Panning for helpful discussions, and AHA (0256225T) and NIH (DK49194) for financial support.

REFERENCES

1 Taylor, C. W., da Fonesca, P. C. A. and Morris, E. P. (2004) IP_3 receptors: the search for structure. Trends Biochem. Sci. **29**, 210–219

2 Patterson, R. L., Boehning, D. and Snyder, S. H. (2004) Inositol 1,4,5-trisphosphate receptors as signal integrators. Annu. Rev. Biochem. **73**, 437–465

3 Wojcikiewicz, R. J. H. (1995) Type I, II, and III inositol 1,4,5-trisphosphate receptors are unequally susceptible to down-regulation and are expressed in markedly different proportions in different cell types. J. Biol. Chem. **270**, 11678–11683

4 Taylor, C. W., Genazzani, A. A. and Morris, S. A. (1999) Expression of inositol trisphosphate receptors. Cell Calcium **26**, 237–251

5 Yamamoto-Hino, M., Sugiyama, T., Hikichi, K., Mattei, M. G., Hasegawa, K., Sekine, S., Sakurada, K., Miyawaki, A., Furuichi, T., Hasegawa, M. and Mikoshiba, K. (1994) Cloning and characterization of human type 2 and type 3 inositol 1,4,5-trisphosphate receptors. Receptor Channels **2**, 9–22

6 Yamada, N., Makino, Y., Clark, R. A., Pearson, D. W., Mattei, M. G., Guenet, J. L., Ohama, E., Fujino, I., Miyawaki, A., Furuichi, T. and Mikoshiba, K. (1994) Human inositol 1,4,5-trisphosphate receptor, $InsP_3R1$: structure, function, regulation of expression and chromosomal location. Biochem. J. **302**, 781–790

7 Blondel, O., Takeda, J., Janssen, H., Seino, S. and Bell, G. I. (1993) Sequence and functional characterization of a third inositol trisphosphate receptor subtype, IP3R3, expressed in pancreatic islets, kidney, gastrointestinal tract, and other tissues. J. Biol. Chem. **268**, 11356–11363

8 Wojcikiewicz, R. J. H. and Luo, S. G. (1998) Differences among type I, II, and III inositol 1,4,5-trisphosphate receptors in ligand-binding affinity influence the sensitivity of calcium stores to inositol 1,4,5-trisphosphate. Mol. Pharmacol. **53**, 656–662

9 Tu, H., Wang, Z., Nosyreva, E., De Smedt, H. and Bezprozvanny, I. (2005) Functional characterization of mammalian inositol 1,4,5-trisphosphate receptor isoforms. Biophys. J. **88**, 1046–1055

10 Maes, K., Missiaen, L., Parys, J. B., De Smet, P., Sienaert, I., Waelkens, E., Callewaert, G. and De Smedt, H. (2001) Mapping of the ATP-binding sites on inositol 1,4,5-trisphosphate receptor type 1 and type 3 homotetramers by controlled proteolysis and photoaffinity labeling. J. Biol. Chem. **276**, 3492–3497

11 Tu, H., Wang, Z. and Bezprozvanny, I. (2005) Modulation of mammalian inositol 1,4,5-trisphosphate receptor isoforms by calcium: a role of calcium sensor region. Biophys. J. **88**, 1056–1069

12 Wojcikiewicz, R. J. H. and Luo, S. G. (1998) Phosphorylation of inositol 1,4,5-trisphosphate receptors by cAMP-dependent protein kinase. Type I, II, and III receptors are differentially susceptible to phosphorylation and are phosphorylated in intact cells. J. Biol. Chem. **273**, 5670–5677

13 Dyer, J. L., Mobasheri, H., Lea, E. J. A., Dawson, A. P. and Michelangeli, F. (2003) Differential effect of PKA on the Ca^{2+} release kinetics of the type I and III $InsP_3$ receptors. Biochem. Biophys. Res. Commun. **302**, 121–126

14 Giovannucci, D. R., Groblewski, G. E., Sneyd, J. and Yule, D. I. (2000) Targeted phosphorylation of inositol 1,4,5-trisphosphate receptors selectively inhibits localized Ca^{2+} release and shapes oscillatory Ca^{2+} signals. J. Biol. Chem. **275**, 33704–33711

15 Ferris, C. D., Cameron, A. M., Bredt, D. S., Huganir, R. L. and Snyder, S. H. (1991) Inositol 1,4,5-trisphosphate receptor is phosphorylated by cyclic AMP-dependent protein kinase at serines 1755 and 1589. Biochem. Biophys. Res. Commun. **175**, 192–198

16 Haug, L. S., Jensen, V., Hvalby, O., Walaas, S. I. and Ostvold, A. C. (1999) Phosphorylation of the inositol 1,4,5-trisphosphate receptor by cyclic nucleotide-dependent kinases *in vitro* and in rat cerebellar slices *in situ*. J. Biol. Chem. **274**, 7467–7473

17 Soulsby, M. D., Alzayady, K., Xu, Q. and Wojcikiewicz, R. J. H. (2004) The contribution of serine residues 1588 and 1755 to phosphorylation of the type I inositol 1,4,5-trisphosphate receptor by PKA and PKG. FEBS Lett. **557**, 181–184

18 Wagner, II, L. E., Li, W., Joseph, S. K. and Yule, D. I. (2004) Functional consequences of phosphomimetic mutations at key cAMP-dependent protein kinase phosphorylation sites in the type 1 inositol 1,4,5-trisphosphate receptor. J. Biol. Chem. **279**, 46242–46252

19 Bruce, J. I. E., Shuttleworth, T. J., Giovannucci, D. R. and Yule, D. I. (2002) Phosphorylation of inositol 1,4,5-trisphosphate receptors in parotid acinar cells. A mechanism for the synergistic effects of cAMP on Ca^{2+} signaling. J. Biol. Chem. **277**, 1340–1348

20 Straub, S. V., Giovannucci, D. R., Bruce, J. I. E. and Yule, D. I. (2002) A role for phosphorylation of inositol 1,4,5-trisphosphate receptors in defining calcium signals induced by peptide agonists in pancreatic acinar cells. J. Biol. Chem. **277**, 31949–31956

21 Kennelly, P. J. and Krebs, E. G. (1991) Consensus sequences as substrate specificity determinants for protein kinases and protein phosphatases. J. Biol. Chem. **266**, 15555–15558

22 Fagan, K. A., Mahey, R. and Cooper, D. M. F. (1996) Functional co-localization of transfected Ca^{2+}-stimulable adenylyl cyclases with capacitative Ca^{2+} entry sites. J. Biol. Chem. **271**, 12438–12444

23 Iwai, M., Tateishi, Y., Hattori, M., Mizutani, A., Nakamura, T., Futatsugi, A., Inoue, T., Furuichi, T., Michikawa, T. and Mikoshiba, K. (2005) Molecular cloning of mouse type 2 and type 3 inositol 1,4,5-trisphosphate receptors and identification of a novel type 2 receptor splice variant. J. Biol. Chem. **280**, 10305–10317

24 Yoshikawa, F., Iwasaki, H., Michikawa, T., Furuichi, T. and Mikoshiba, K. (1999) Trypsinized cerebellar inositol 1,4,5-trisphosphate receptor. Structural and functional coupling of cleaved ligand binding and channel domains. J. Biol. Chem. **274**, 316–327

25 Perona, J. J. and Craik, C. S. (1997) Evolutionary divergence of substrate specificity within the chymotrypsin-like serine protease fold. J. Biol. Chem. **272**, 29987–29990

26 Tu, H., Tang, T., Wang, Z. and Bezprozvanny, I. (2004) Association of type 1 inositol 1,4,5-trisphosphate receptor with AKAP9 (Yotiao) and protein kinase A. J. Biol. Chem. **279**, 1–8

Received 12 August 2005; accepted 18 August 2005
Published as BJ Immediate Publication 18 August 2005, doi:10.1042/BJ20051325